Dynamical Analysis of Coastal Lee Waves observed in AVHRR Images

Xiaofeng Li [1], Quanan Zheng [2], William G. Pichel[1], Xiao-Hai Yan [2], W. Timothy Liu[3], Pablo Clemente-Colón[1]

[1]NOAA/NESDIS, E/RA3, Room 102, WWBG, 5200 Auth Road,
Camp Springs, MD 20746-4304, U.S.A.
Xiaofeng.Li@noaa.gov

[2]College of Marine Studies, University of Delaware, Newark, DE 19716, U.S.A.
zheng@triton.cms.udel.edu

[3] Jet Propulsion Laboratory
300-323, California Institute of Technology,
Pasadena, CA 91109, U.S.A.

Abstract. We examine a group of wave-like cloud patterns that occurred along the coast of Texas on two consecutive NOAA (National Oceanic and Atmospheric Administration) satellite AVHRR (Advanced Very High Resolution Radiometer) IR (infrared) images taken on January 22, 1999. These wave-like cloud patterns were interpreted to be signatures of a coastal lee wave packet on the basis of simultaneous field observations and coastal lee wave theories [Zheng *et al.*, 1998a]. The wave packet contains 13 waves with crest lines generally parallel to the coastline. The lengths of leading wave crest lines are longer than 500 *km*. The average wavelength is 9.5 *km* ranging from 6.2 to 14.7 *km*. The width of the horizontal distribution band of the wave packet is as wide as 113 *km*. This case represents the most energetic coastal lee wave packet that has ever been reported.

1. Introduction

The coastal lee wave is a small-scale atmospheric gravity wave occurring along the lee side of a coast as defined by Zheng *et al.*, [1998a]. Formally, these waves are analogous to mountain lee waves [e.g., Gjevik and Marthinsen, 1978] and lee waves induced by isolated islands [e.g., Mitchell *et al.*, 1990; Vachon *et al.*, 1994; Li *et al.*, 1998]. Lee waves are frequently imaged by the visible and infrared (IR) channels of AVHRR onboard the NOAA (National Oceanic and Atmospheric Administration) series of Polar-orbiting Operational Environmental Satellites (POES) as wave-like cloud patterns [Gjevik and Marthinsen, 1978; Mitchell *et al.*, 1990]. Over the ocean, wind speed fluctuations at the sea surface associated with the lee waves modulate the sea surface roughness, and thus lee waves can also be imaged by Synthetic Aperture Radar (SAR) through the resonant or Bragg scattering mechanism. By analyzing the wave-like patterns on SAR images, information on lee wave dynamics can be retrieved [Vachon *et al.*, 1994; Zheng *et al.*, 1998a].

The first reported case of coastal lee wave observation with SAR is an ERS-1 (European Remote Sensing Satellite) SAR image along the western coast of Taiwan Strait [Zheng *et al.*, 1998a]. The waves occurred as wave packets containing 6-17 waves and were characterized by crest lines that were generally parallel to the coastline with crest lengths from 20 to 80 *km* and wavelengths ranging from 1.7 to 4.2 *km* with an average of 3 *km*. It was verified by a physical model that the sea/land breeze circulation driven by the land-sea temperature difference [Simpson, 1994] was an important coastal lee wave generation mechanism.

A similar case of atmospheric wave packets was reported in an offshore area near the Pakistani coast from space shuttle photographs taken on April 29, 1993 [Zheng *et al.*, 1998b]. The packet contained 19 waves with an average wavelength of 1 *km* and a crest line longer than 250 *km*. The packet had highly nonlinear characteristics and was categorized in the morning glory family, as observed previously in northern Australia [Clarke, 1972; , 1988]. The land breeze and katabatic flow were believed to be possible generation mechanisms.

In this paper, we will provide new evidence concerning the genesis of coastal lee waves. The wave patterns were seen in NOAA satellite AVHRR IR images of January 22, 1999. Simultaneously observed surface boundary conditions reveal that a land breeze circulation existed at the imaging time. The scales of the waves seen in the two images indicate that this wave packet is more energetic than coastal lee waves cases reported previously.

2. Observations

2.1 Interpretation of NOAA AVHRR images

The data used for this study consists of NOAA CoastWatch [Li *et al.*, 2000] AVHRR channel 4 (11 μm) images taken from the NOAA-14 and NOAA-15 POES

satellites. POES satellites operate operationally in a pair to ensure that the data, for any region of the earth, are no more than six hours old. CoastWatch is a NOAA program managed by NESDIS with CoastWatch Regional Nodes located at NOAA laboratories and offices in eight coastal states. Input data for the production of CoastWatch imagery are HRPT (High Resolution Picture Transmission) level 1b data sets. These consist of AVHRR detector output from the five channels of the AVHRR with appended calibration and earth location information. For the US east coast, Great Lakes, and Gulf of Mexico regions, data sets are received from every satellite pass over the Wallops Station, Virginia reception mask. Satellite data from Wallops are transmitted to the NESDIS Central Environmental Satellite Computer System (CEMSCS) in Suitland, Maryland as soon as each satellite overpass is completed. Processing into level 1b products proceeds automatically as soon as the complete pass has been received, followed by CoastWatch mapping over each region covered by the satellite pass. All AVHRR five channels (visible channels 1 & 2 at 0.6 and 0.9 μm; short-wavelength IR channel 3 at 3.7 μm; and long-wavelength IR channels 4 & 5 at 11 and 12 μm) are mapped to a series of 'sector' images from the region maps. These sector maps are 512 × 512 pixels in size for selected areas within the region. Sectors are produced at near full-resolution, approximately 1.3 *km*/pixel at 30°N latitude (AVHRR full resolution is 1.1 *km* at nadir).

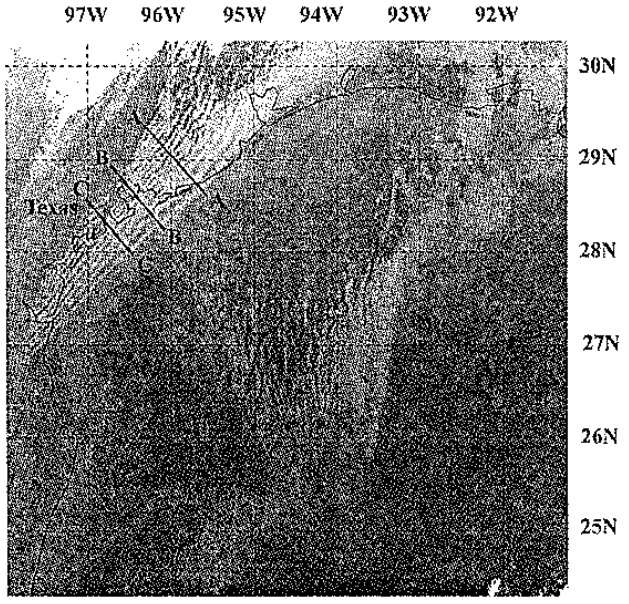

Figure 1. NOAA-14 AVHRR IR image of the northwestern Gulf of Mexico and adjacent coastal regions received at 09:33 Z (a, coded 0933) on January 22, 1999. Image resolution is approximately 1.3 *km*. Alternative dark-bright cloud patterns along the coast are interpreted to be signatures of coastal lee waves.

The AVHRR IR image containing the wave-like cloud patterns is shown in Figure 1. The image was taken at 09:33 Z on January 22, 1999 by NOAA-14 satellite; and another image with wave pattern was taken at 14:21 Z on the same day by NOAA-15 (not shown here). For simplicity, the two images will be coded hereafter as 0933 and 1421, respectively. The images cover the area from 24°17' to 30°17' N latitude and from 91°13' to 97°58' W longitude, which includes the northwestern Gulf of Mexico, part of the Mexico, all of the Texas, and the most of the Louisiana coastal regions.

Both images are from AVHRR channel 4. Therefore, the gray levels in the image represent the average brightness temperature within each resolution cell. In this case, the higher temperatures are represented by darker grey values and low temperatures by lighter grey values. The plume-like patterns in white and light gray are cloud patterns.

On image 0933, we can see that the clouds along the coast appear as alternating bright and dark bands, in a wave-like pattern. We assume that the pattern represents a packet of atmospheric waves. The packet contains 13 waves distributed in a band with width of 113 *km*. The wavelength ranges from 6.2 to 14.7 *km* with an average of 9.5 *km*. The crest line of leading waves inside the image is as long as 532 *km*. After nearly 5 hours, the packet moved eastward with the front centered at 29°00' N, 93°00' W, as shown in image 1421, and the cloud patterns appeared rather vague compared with image 0933, implying that the waves had decayed. Only 8 waves survived. The crest line decreased by 58% to 224 *km*, and the distribution band decreased by 51% to 55 *km*. The average wavelength decreased by 23% to 7.3 *km*. By comparing the wave patterns on the two images, we conclude that the decrease in average wavelength was caused by the leading waves with large wavelengths being lost, possibly due to wave breaking. In image 0933, the average wavelength of the rear 8 waves in the packet is also 7.3 *km*. Therefore, the waves with smaller wavelengths were relatively stable, and most likely non-dispersive in character. We examined the images received prior to 0933 and 1421, however, there were no wave-like patterns found. The AVHRR image taken at 20:58Z (not shown here) did not contain a wave pattern, implying that the life span of the wave packet was on the order of 10 hours. The interpretation results are shown in Figure 2.

2.2. Surface boundary conditions

a. Field Observations

We obtained winds and air temperatures measured at nearby buoy stations (42020 and 42035) and Coastal-Marine Automated Network (C-MAN) stations (PTAT2 and SRST2), as shown in Figure 2.

We see that the average air temperatures measured by

the buoys were about 2 to 4°C higher than measured over the land by the C-MAN stations along the coast prior to the imaging time. This rather large land-sea temperature difference is favorable for sea/land breeze circulation development [Simpson, 1994; Zheng *et al.*, 1998a].

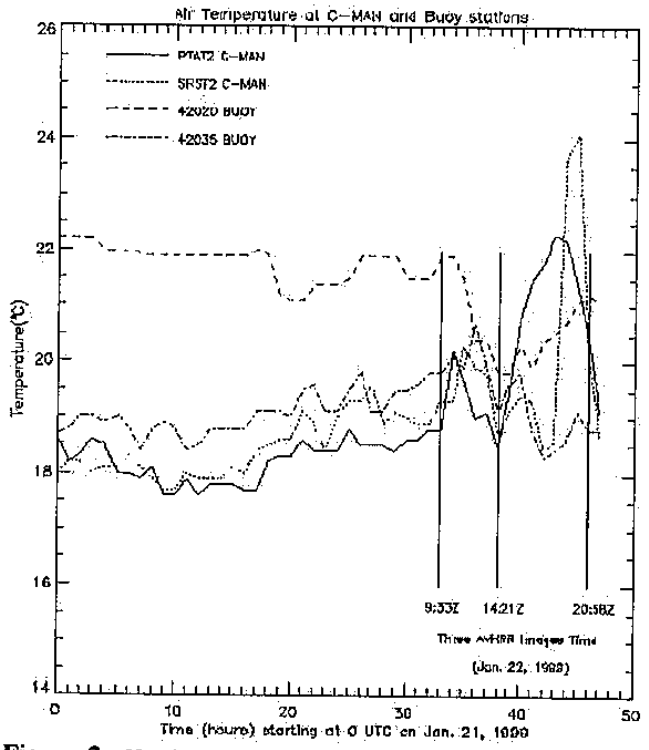

Figure 2 Hourly average sea surface air temperature measured at buoys 42020 (dashed line) and 42035 (dash dot line) and land surface air temperature measured at C-MAN stations PTAT2 (solid line) and SRST2 (dotted line).

The ten-minute average wind speed and direction measured at the two C-MAN stations show that both wind speed and direction were changing when the 0933 image was taken. At the PTAT2 station, the wind speed changed from 15 ms^{-1} to 2 ms^{-1} and the wind direction changed from 165° to 245° (clockwise from north) within 30 minutes. Over the same period, similar changes were also observed at the SRST2 station with the wind speed dropping from 13 ms^{-1} to 10 ms^{-1} and direction changing from 155° to 255°. On average, the wind vector changed from (14 ms^{-1}, 160°) to (6 ms^{-1}, 250°) during the passage of the front.

b. Radiosonde Observations

A radiosonde instrument consists of sensors for the measurement of pressure, temperature, relative humidity and velocity.

The nearest radiosonde station to the study region is located at Corpus Christi, Texas (27°34.8' N, 97°13.0' W). The wave shown in Figure 1 passed this station three hours prior to the radiosonde deployment. The virtual and dew point temperature profiles, measured at 1200 Z on January 22, 1999, show that the virtual temperature, ΔT, was small between the 970 and 850 *mb* levels, but increased above. This indicates that clouds existed from the 970 to 850 *mb* levels (ΔT minimum). The wind between 970 and 850 *mb* was uniform at 21 knots (10.8 ms^{-1}) from 300°.

It is feasible to estimate the cloud top height by using the temperature measured by the AVHRR IR channel. In this case, the cloud top temperature across the wave pattern on the AVHRR channel 4 image varies from 284.5° to 292.5° *K*. By comparing with the radiosonde profile, we found that these temperatures correspond to the 850 *mb* level, which is the bottom altitude of a strong atmospheric inversion layer. Therefore, it is reasonable to conclude that the wave occurred below the 850 *mb* level.

3. Dynamical Analysis

3.1 Genesis

The above data indicate that the average wavelength and crest line length of the atmospheric waves under investigation are as large as 9.5 *km* and 500 *km*, respectively. Both parameters are far beyond the range of previously reported coastal lee wave cases [Zheng *et al.*, 1998a, 1998b]. The wavelength scale is close to typical mountain lee wave wavelengths of 10 *km* [Gossard and Hooke, 1975; Panchev, 1985]. The airflow lift caused by a mountain obstacle is a key mechanism for generating a mountain lee wave. However, given the topography, it is unreasonable to interpret these waves as mountain lee waves. Examining the geomorphologic features of the study area, we see that conditions are not favorable for generation of mountain lee waves.

The region covered by the wave-like clouds includes the coastal plain of the Gulf of Mexico. The nearest feature that is steep enough to force an upward airflow, is the Balcones Escarpment, the eastern border of Edward Plateau, located around 200 *km* inland from the coast. Mountain lee waves are generally stationary with respect to a mountain, i.e., they are standing. As will be discussed, physically, the observed waves may be stationary waves, but with respect to the atmospheric front rather than the land. It is reasonable, therefore, to conclude that the waves are not mountain lee waves.

We assume that the observed waves are coastal lee waves, although they are much stronger than the previously reported cases. The physical model developed by Zheng *et al.* [1998a] shows that the land breeze circulation, which is driven by the land-sea temperature difference, is an important mechanism for generating coastal lee waves. In our case, the surface boundary conditions indicate that this is also true. The observed

waves occurred in the middle latitudes (from 27° to 30° N latitude) during the local early winter. The land-sea temperature difference reaches a maximum value during this season. The measurements shown in Figure 2 reveal that the sea surface air temperature was 2° to 4° *C* higher than the land surface air temperature before the waves occurred, implying a favorable condition for generating the land breeze. On the other hand, the observations of wind speed and wind direction recorded at the C-MAN stations show that the original wind vector prior to the front passage is (14 ms^{-1}, 160°), while the wind vector after the front passage is (6 ms^{-1} from 250°). Therefore, using the vector analysis method, we can see that a wind vector of (15 ms^{-1} from 319°) existed during the front passage. Compared with the map, we see that this wind vector is oriented across the coastline. This indicates that a land breeze circulation with a wind speed of 15 ms^{-1} and wind direction of 319° had been established and played a key role in generation of the observed waves. This surface wind vector is in good agreement with upper air radiosonde wind measurement below the inversion layer (i.e., 10.8 ms^{-1} from 300° for the 970 to 850 *mb* level).

3.2 Wave forms

To better determine the nature of the observed waves, we will compare the observed wave forms with a theoretical model. Zheng *et al.* [1998a] developed a two-dimensional physical model and obtained an analytical form for the coastal lee wave solution. In their model, the *x*-axis is perpendicular to the coastline, positive shoreward. The *z*-axis is perpendicular to the sea surface, positive upward. The origin is located at the land breeze front. The system is horizontally divided into two regions from the front at $x = 0$. The land breeze and vertical stratification occurs for $x > 0$. The model atmosphere has three layers. The upper layer has an infinite depth, while the lower layer containing the land breeze, has a depth of *H*. There is a transition-layer with a thickness of $2\Delta H$ sandwiched between the two layers. The model may be considered to be a small scale, linear system.

Coastal lee wave can be expressed in the following form [Gossard, 1974]:

$$w = \frac{u_0 Hsinh(kz)}{Lsinh(kH)} sech^2(\frac{x}{L}) \exp[i(kx - \sigma t)] \qquad (1)$$

where u and w represent the horizontal and vertical components of the wind velocity, and k ($= 2\pi/\lambda$, where λ is the wavelength.) represents the wavenumber. The amplitudes of the wind speeds in the two layers appear to be the same, u_0. L is the characteristic length of the frontal zone, σ is the angular frequency, and we take only the real part.

The vertical amplitude of the wave, η, can be calculated from:

$$\eta = \int_0^{T/4} w \, dt \qquad (2)$$

where T is the period of waves. Substituting (1) into (2) yields

$$w = \frac{u_0 Hsinhkz}{LsinhkH} sech^2(\frac{x}{L}) \exp[i(kx - \sigma t)]., \qquad (3)$$

where again, only the real part is to be taken. In this case, the spatial characteristic scale of waves is $\underline{L} = O(10\ km)$, the characteristic velocity is $\underline{U} = O(15\ ms^{-1})$, so that the Rossby number ε ($=\underline{U}/f\underline{L}$) is 15, which is much greater than 1. The motion is still at a small scale. Therefore, the governing equations written above are still valid. The wave amplitudes are related to the cloud top temperatures of the wave-like cloud patterns, which are measurable in the AVHRR IR images. Since the clouds are thick and opaque, the AVHRR channel 4 brightness temperature is essentially equal to the actual cloud top temperature [Mitchell *et al.*, 1990]. Therefore, the pressure fields associated with the cloud top temperatures can be converted from the radiosonde measurement. We then converted the pressure field to altitude by using the hypsometric formula:

$$H = \frac{RT_0}{Mg}(\ln P_H - \ln P_0) \qquad (4)$$

where H is the altitude above sea level in *m*, g is the gravitational acceleration, 9.8 ms^{-2}, the molecular weight of air, M, is 28.9644 $g\ mol^{-1}$, the molar constant of gas, R, is 8.3143 $Jmol^{-1}K^{-1}$, and T_0 is the virtual temperature in *K*, and P_H and P_0 are the pressures in *mb* at altitude H and at sea level, respectively. Comparisons of the model coastal lee wave (3) at $z = H$, with the wave forms derived from profiles A-A in Figure 1, is shown in Figure 3.

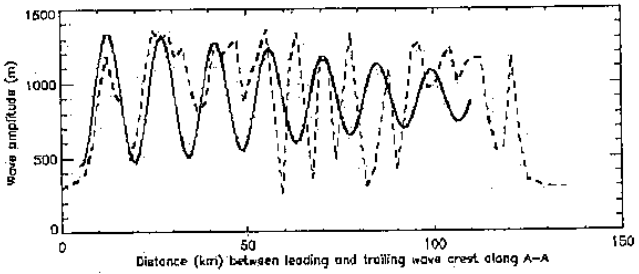

Figure 3. Comparisons of wave forms measured along lines A-A marked in Figure 1 with theoretical model of coastal lee waves.

We see that the observed waves are reasonably well simulated by the theoretical model, especially for the first four leading waves. For the trailing waves, the model provides an explanation for the amplitude decay, but does not explain the shortening of wavelengths. This discrepancy likely reflects the nonlinear features of the observed waves, which cannot be described accurately with a linear wave model.

Since we can not determine whether the temperature within the wave trough region (non-cloudy band) was the atmosphere or the land surface, it is not feasible to estimate the wave amplitude from the satellite images alone. In Figure 3, only the wave crests are plotted at their approximate altitude.

3.3 Dispersion relation

The dispersion for the coastal lee waves can be derived from a quartic equation [Gossard and Hooke, 1975]:

$$\left(\frac{C}{u0}\right)^4 - \left[1 + \frac{(2\alpha - 1)^2 - e^{-4\alpha}}{4\alpha^2} + \frac{R}{\alpha}\right]\left(\frac{C}{u0}\right)^2 + \left(\frac{1+R}{2\alpha} - 1\right)^2 - \left(\frac{1+R}{2\alpha}\right)^2 e^{-4\alpha} = 0 \quad (5)$$

where C is the phase speed, $\alpha = k\Delta H$, and R ($=\Delta\rho g \Delta H/\rho_0 u_0^2$) is the Richardson number. In our case, λ= 9.5 *km*, ΔH is chosen as $\lambda/2\pi$ ($\approx$1.5 *km*), $\Delta\rho/\rho_0$ = 0.013, g = 9.8 ms^{-2}, and u_0 = 15 ms^{-1}. Thus, there are two real solutions:

$$C_1 = 0.09u_0 \quad (6)$$

$$C_2 = 1.38u_0 \quad (7)$$

From Eq. (6), we conclude that the group speed is so small that we can consider that

$$C_g = 0 \quad (8)$$

This implies that the coastal lee waves may exist as stationary waves with respect to the atmospheric front. In an absolute reference frame that is fixed to the Earth's surface, the wave velocity is

$$\vec{U} = \vec{U}_0 + \vec{C}, \quad (9)$$

where $\vec{U}_0$ is the velocity of the moving reference frame. If $\vec{U}_0 = U_0\vec{i}$ for simplicity, the group speed observed in the absolute system is:

$$C_g = U_0. \quad (10)$$

This implies that the waves move in step with the moving front. The behavior of the coastal lee wave packet is consistent with this. The surface observations and AVHRR images show that when the front moved seaward into the Gulf of Mexico, pushed from behind by the low-pressure system, the waves followed the front's movement. On the other hand, from the two AVHRR images, we calculated that the average velocity of the front movement was 10.6 ms^{-1}, which coincides with the land breeze circulation velocity derived from observations with the vector analysis method. The radiosonde velocity measurement also agreed with the observation. The average wind speed at the 850 *mb* was measured to be (10.8 ms^{-1} from 300°). Therefore, the front moves with the wind.

The second solution gives a large phase speed, which represents a fast propagating coastal lee wave. This solution, however, does not agree with our observations.

4. Conclusions and Discussion

Wave-like cloud patterns in NOAA AVHRR images taken over the Texas coastal region on January 22, 1999 were interpreted to be signatures of coastal lee waves, a type of small-scale atmospheric gravity wave. The waves occurred in the form of a wave packet containing 13 waves with an average wavelength of 9.5 *km*. The crest lines were generally parallel to the coastline with the crest length of the leading wave longer than 500 *km*. The average group velocity was 10.6 ms^{-1} with respect to the Earth's surface, as measured from two consecutive images. The life span of the event was estimated to have been on the order of 10 hours. Simultaneous field observations show that the sea surface air temperature was 2° to 4°*C* higher than the land surface air temperature prior to the imaging time, constituting a favorable condition for driving a land breeze circulation. Time series of wind data measured at two C-MAN stations beneath the cloud patterns indicate a significant change in the wind speed and wind direction, implying that the land breeze circulation had been established simultaneously with the wave packet. The wave form and propagation of the observed waves are comparable with a theoretical model of the coastal lee waves.

The estimated vertical velocity of airflow induced by the coastal lee waves under investigation may reach 0.3 ms^{-1}. The amplitudes of the waves may reach 1 *km* as shown in Figure 3. This means that the waves may constitute a powerful disturbance for objects flying in the lower atmosphere, and some aircraft crashes happening along the coast may be related to this type of disturbance. The results of this study indicate that NOAA satellites are capable of providing visual and near real-time images of the waves, which can be used as a baseline for forecasting and research. On the basis of these results, we conclude that the observed case provides new evidence for the occurrence of coastal lee waves along the US coast.

Acknowledgment This work was supported by the NOAA/NESDIS Ocean Remote Sensing Program, and was partially supported by NASA NSCAT and EOS Interdisciplinary Science Investigations programs, the NASA JASON program through grant NAG5-7949, the NOAA Sea Grant Program through grants NA96RG0029, and NSF PFF OCE-9453499. Radiosonde data were downloaded from the University of Wyoming Atmosphere Science Department web site at http://www-das.uwyo.edu/upperair.

References

Clarke, R. H., The morning glory: an atmospheric hydraulic jump, *J. Appl. Meteor.*, 11, 304-311, 1972.

Gjevik B., and T. Marthinsen, Three-dimensional lee-waves pattern, *Quart. J. R. Met. Soc.*, 104, 947-957, 1978.

Gossard, E. E., Dynamic stability of an isentropic shear layer in a statically stable medium, *J. Atmos. Sci.*, 31, 488-492, 1974.

Gossard, E. E., and W. H. Hooke, *Waves in the Atmosphere*, Elsevier Scientific Publishing Co., New York, pp. 1-456, 1975.

Li, X., W. G. Pichel, K. S. Friedman, and P. Clemente-Colón, The sea surface imprint of island lee waves as observed by RADARSAT synthetic aperture radar, *Proc. of the IEEE International Geoscience and Remote Sensing Symposium*, 763-766, 1998.

Li, X., W. Pichel, P. Clemente-Colón, V. Krasnopolsky, and J. Sapper, Validation of coastal sea and lake surface temperature measurements derived from NOAA/AVHRR data, *International Journal of Remote Sensing*, in press, 2000.

Mitchell, R. M., R. P. Cechet, P. J. Turner, and C. C. Elsum, Observation and interpretation of wave clouds over Macquarie Island, *Quart. J. R. Met. Soc.*, 116, 741-752, 1990.

Panchev, S., *Dynamic Meteorology*, D. Reidel Publishing Co., Boston, pp. 1-360, 1985.

Simpson, J. E., *Sea breeze and local winds*, Cambridge University Press, Cambridge, pp. 1-234, 1994.

Smith, R. K., Traveling waves and bores in the lower atmosphere: the 'morning glory' and related phenomena, *Earth-Sci. Rev.*, 25, 267-290, 1988.

Vachon, P. W., O. M. Johannessen, and J. A. Johannessen, An ERS 1 synthetic aperture radar image of atmospheric lee waves, *J. Geophys. Res.*, 99, 22, 483-22,490, 1994.

Zheng, Q., X.-H. Yan, V. Klemas, C.-R. Ho, N.-J. Kuo, and Z. Wang, Coastal lee waves on ERS-1 SAR images, *J. Geophys. Res.*, 103, 7979-7993, 1998a.

Zheng, Q., X.-H. Yan, W. T. Liu, V. Klemas, D. Greger, and Z. Wang, A solitary wave packet in the atmosphere observed from space, *Geophys. Res. Lett.*, 25, 3559-3562, 1998b.